

Cluster calculations of ZnO with Cu and Ni impurities

Wanda V. M. Machado, Dina L. Kinoshita, and Luiz G. Ferreira
Instituto de Física, Universidade de São Paulo, Caixa Postal 20 516, 01 498 São Paulo, Brazil

Manoel L. DeSiqueira
Instituto de Ciências Exatas, Universidade Federal de Minas Gerais, Caixa Postal 702, 30 000 Belo Horizonte, Brazil
 (Received 11 September 1989)

The variational cellular method, extended to study crystalline structures, has been applied to 17-atom clusters representing a ZnO crystal without and with substitutional impurities. Self-consistent-field electronic-structure calculations were carried out for the substitutional Cu and Ni. The (2+)-charge ion states were studied and the optical transitions discussed in terms of Koopmans's theorem or transition-state calculations, depending on their range of applicability. The analysis of the results is preceded by a discussion on the general questions of to what extent a cluster can be used to calculate crystal energy bands and localized states.

I. INTRODUCTION

The aim of this work is to analyze from the theoretical point of view the behavior of Cu and Ni impurities in the ZnO semiconductor. The linearized variational cellular method¹⁻¹⁰ (VCM) is used to compute the electronic structure of these substitutional 3*d* transition-metal impurities.

ZnO is a II-VI compound with a large band gap (3.4 eV),¹¹ enough to place it in the vicinity of insulating materials. It is also commonly placed in an intermediate position between ionic and covalent solids.¹² It has a hexagonal wurtzite structure in which the tetrahedra are slightly distorted in the [111] direction.¹³ Rossler¹⁴ showed that the difference between the wurtzite and zinc-blende structures of ZnO is just the small splitting of the degenerate levels of the cubic arrangement. The conduction and valence bands of ZnO have been studied by optical techniques^{15,16} which show that both extrema are at the center of the Brillouin zone. The upper valence bands are mainly derived from the O 2*p* states, while the lowest conduction band is primarily made out of the atomic Zn 4*s* state.^{14,17,18} The Zn core 3*d* band lies below the C 2*p* band¹⁴ but there is mixing (hybridization) between the two bands.

Impurity states in zinc oxide semiconductors doped with Cu or Ni have been investigated by luminescence and absorption experiments.¹⁹⁻²⁶ These impurity centers display the well-known infrared absorption commonly assigned to an internal 3*d* transition of a doubly-positive impurity charge state. ZnO:Cu and ZnO:Ni also have a green luminescence that corresponds to a hole transfer from the *d* shell of the divalent impurity to an acceptor state, supposed to be near the top of the valence band.^{22,26}

II. VARIATIONAL CELLULAR METHOD APPLIED TO CRYSTALS

The variational cellular method was first proposed as a local-density-approximation scheme for the calculation of

the electronic structure of polyatomic systems,¹⁻⁶ and then extended to study crystalline structures through the crystalline cluster technique.⁷⁻¹⁰ The method, which was used to study ZnS (Ref. 9) and ZnS:Cu (Ref. 10) crystals, has several advantages, including the possibility of introducing a common energy reference for the "perfect"- and "defect"-cluster calculations, making it possible to compare the two sets of eigenvalues.

According to the original variational cellular method,¹ the space is partitioned into cells characterized by two parameters γ_i and R_i , so that a point \mathbf{r} belongs to cell i if

$$\gamma_i(\mathbf{r}-\mathbf{a}_i)^2 - \gamma_i R_i^2 < \gamma_j(\mathbf{r}-\mathbf{a}_j)^2 - \gamma_j R_j^2 \quad (1)$$

for any j , where \mathbf{a}_i is the vector position of the center of cell i . The space is thus divided into cells with different shapes that can be adapted to the specific problem. For the inner cells we choose $\gamma_i = \gamma_j > 0$ and the cell boundaries are planes. For a cluster or a molecule one chooses an outer cell for which $\gamma_{\text{out}} < 0$.

Inside each cell, the one-electron wave function $\psi_\alpha(\mathbf{r})$ for state α , and the Coulomb potential $c(\mathbf{r})$ are expanded in spherical harmonics. A spherical average of squared wave functions defines a model number density through

$$n(r) = \left[\sum_{\alpha} \psi_{\alpha}^*(\mathbf{r}) \psi_{\alpha}(\mathbf{r}) \right]_{\text{sph. av.}} \quad (2)$$

and a spherical average of the Coulomb potential plus the exchange-correlation term $\delta E_{xc}/\delta n(r)$ defines the Schrödinger-equation potential $V(r)$:

$$V(r) = [c(\mathbf{r})]_{\text{sph. av.}} + \frac{\delta E_{xc}}{\delta n(r)}. \quad (3)$$

The total energy of the system is written as a functional of $\psi_\alpha(\mathbf{r})$, $c(\mathbf{r})$, $n(r)$, and $V(r)$, and is stationary for variations on these four functions.

In the crystalline cluster method,⁹ one uses the cluster to solve the Schrödinger equation for the many occupied states. The resulting number density is transferred to an infinite lattice, where it is repeated periodically. Then the Poisson equation for the periodic number density is

solved and the resulting potential is transferred back to the cluster until self-consistency is achieved. In our application of this simple idea, the number density and potential of the infinite lattice are put in the muffin-tin format, so that the transference back and forth from the cluster is unambiguous. Due to the linearization of VCM, described in Ref. 6, the whole procedure is fast, allowing the study of many different situations even in our modest computation facilities (a Burroughs 7900 computer).

The self-consistent calculation for the impurity is made with a potential calculated in each iteration as

$$V = V(\text{impure cluster}) - V(\text{pure cluster}) + V(\text{crystal}) \quad (4)$$

where $V(\text{crystal})$ is the self-consistent potential for the crystalline cluster, $V(\text{pure cluster})$ is the potential obtained when the Poisson equation is solved in the cluster, not in the crystal, and $V(\text{impure cluster})$ is the cluster potential calculated when the impurity is introduced into the cluster. So, the calculation of the impurity is a self-consistent cluster calculation made in the presence of the external potential

$$V(\text{crystal}) - V(\text{pure cluster})$$

which converts the impurity in the cluster into an impurity in the crystal. The cluster potentials are non-muffin-tin, but the crystal potential is muffin tin by construction.

III. THE CLUSTER METHOD— LIMITATIONS AND INTERPRETATIONS

To understand our results for ZnO with Cu and Ni impurities, we must first understand in what sense the cluster method can be used instead of the full machinery of a band Green-function calculation. First of all, it is possible to define the ideal cluster. Let $|n, l\rangle$ represent a Wannier state of band n , centered at the lattice site l . The ideal cluster would have a potential

$$V(\text{ideal cluster}) = V(\text{crystal}) + V_0 \sum_n \sum_{|l| > R} |n, l\rangle \langle n, l| \quad (5)$$

where, in the second term, we sum over the Wannier states centered outside the cluster and over the bands we want to study. Though the second term is not commuting with the one-electron Hamiltonian, it is band preserving, that is, it commutes with the projection operator of the bands. Assuming that V_0 is a large positive number, the energy spectrum corresponding to such potential is made of discrete levels constructed out of the Wannier states interior to the cluster ($|l| < R$). Thus the spectrum samples the energy bands of the crystal as shown in Fig. 1. Of course, the discrete levels are between the band maximum and minimum, so that we may safely assert that the ideal cluster has larger band gaps and smaller bandwidths than the crystal.

Another important property of the ideal cluster results from the small delocalization of the Wannier states themselves. In fact, the width of the Wannier function

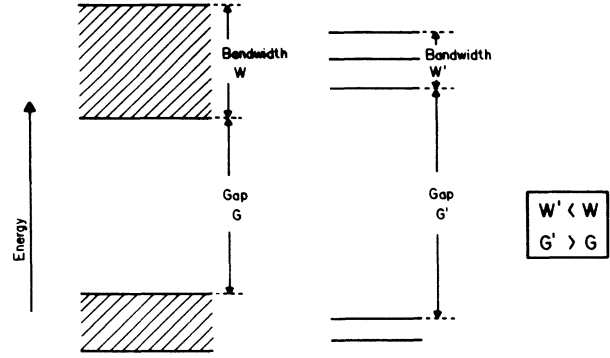


FIG. 1. Schematic representation of the sampling of the energy bands by the energy levels of a cluster. In a cluster calculation, the band gaps are larger and bandwidths smaller.

$$w_n = \left[\int d^3r r^2 a_n(\mathbf{r}) a_n^*(\mathbf{r}) \right]^{1/2} \quad (6)$$

has been calculated²⁷ and shown to be always smaller than the lattice parameter, except for the extremely narrow gap semiconductors. Thus we can say that the external Wannier states ($|l| > R$) make no contribution to the number density in the most internal region of the cluster. Therefore the charge density in the inner region of the cluster may be calculated using those discrete levels pulled from the band and represented by Fig. 1.

In a practical calculation, the ideal cluster of Eq. (5) is not used. Instead one uses a barrier that keeps the eigenfunctions localized. Different cluster schemes present different recipes for the construction of the barrier. What we have been using is the potential most likely to behave as that of Eq. (5), namely,

$$V(\text{practical cluster}) = V(\text{crystal}) + V_0 \Theta(r - R). \quad (7)$$

IV. ENERGY EIGENVALUES AND OPTICAL TRANSITIONS

The one-electron eigenvalue has different meanings in the crystalline VCM results depending on the width of the band that the sample eigenstate represents. The energy eigenvalue ϵ_α is related to the total energy E and the occupation number f_α for the state α by means of²⁸

$$\frac{\partial E}{\partial f_\alpha} = \epsilon_\alpha. \quad (8)$$

On the other hand, first-order perturbation theory states that

$$\frac{\partial \epsilon_\alpha}{\partial f_\alpha} = 2S_\alpha \quad (9)$$

where S_α is the electron self-energy,

$$S_\alpha = \int d^3r \int d^3r' \frac{n_\alpha(\mathbf{r}) n_\alpha(\mathbf{r}')}{|\mathbf{r} - \mathbf{r}'|} + \frac{1}{2} \int d^3r \int d^3r' n_\alpha(\mathbf{r}) \frac{\delta^2 E_{xc}}{\delta n(\mathbf{r}) \delta n(\mathbf{r}')} n_\alpha(\mathbf{r}') \quad (10)$$

given in terms of the number density $n_\alpha(\mathbf{r})$ for the state α and the exchange-correlation functional E_{xc} . The eigenvalue ϵ_α is practically a linear function of the occupation number f_α ,²⁹ then

$$E(f_\alpha) = E(0) + \epsilon_\alpha(0)f_\alpha + S_\alpha f_\alpha^2, \quad (11)$$

$$\epsilon_\alpha(f_\alpha) = \epsilon_\alpha(0) + 2S_\alpha f_\alpha. \quad (12)$$

If $E(-1)$ is the ionic energy, $E(0)$ the energy of the neutral cluster, and $\epsilon_\alpha(-\frac{1}{2})$ the eigenvalue at half-occupation, that is when one-half electron is removed (transition state), then

$$E(-1) - E(0) = -\epsilon_\alpha(0) + S_\alpha, \quad (13)$$

$$\epsilon_\alpha(-\frac{1}{2}) = \epsilon_\alpha(0) - S_\alpha. \quad (14)$$

The two situations of Fig. 2 will be considered.

(a) *Broad bands.* Whatever localized excitation (particle or hole) is created, it is scattered into the band continuum so that the true stationary (quasi) excitations are Bloch states with vanishing number density and self-energy according to Eq. (10). Then the eigenvalue $\epsilon_\alpha(0)$ coincides with the total-energy difference (Koopmans's theorem).

(b) *Narrow bands and localized defect eigenstates.* If the bandwidth is small and the self-energy is large, the localized excitation will fall out of the range of the band and thus cannot be scattered into the band continuum. In this case one measures the energy to create a localized state with its self-energy, and the comparison with experiment has to be made by means of Eq. (14).

A priori we do not know if we are dealing with a broad or narrow band. Hoping that the discrete eigenvalues of the cluster give a reasonable description of the bandwidth, we can compare the self-energy calculated according to Eq. (14) with that width, and decide. In the case of the defect localized states, it is possible that its eigenfunction extends through many atoms.³⁰ A small cluster, by confining the state in a smaller region, might create an artificially larger self-energy. Thus it is advisable to com-

pare experiment with the eigenvalues at full (Koopmans) and half-occupation (transition state).

Finally we mention that, when calculating the transition state for the pure cluster, we must define the self-consistent potential as in Eq. (4). The localized excitation is an "impurity" in the perfect crystal and cannot be repeated periodically in a lattice, as we do with the number density of the ground state cluster.

V. RESULTS AND DISCUSSION

The cluster used consists of a central host cation, or impurity, surrounded by four host anion first neighbors, and 12 host cation second neighbors, placed in a tetrahedral configuration compatible with an undistorted zinc-blende lattice. The parameters of the cells are listed in Table I. The Zn and O radii were chosen between the ionic and covalent values.¹² The deep core states, up to 3p, in Zn, Cu, and Ni were kept within the sphere inscribed in the cell (the wave functions being set equal to zero at the inscribed sphere radius), and so were the 3d electrons of the outermost shell of Zn atoms. According to this model, the cluster $\text{ZnO}_4\text{Zn}_{12}$ has a total of 42 valence electrons, 32 filling the sp^3 hybrids, and ten filling the 3d bands of the central cation.

Table II shows the clusters that were calculated to describe the optical properties of ZnO, ZnO:Cu, and ZnO:Ni. Cluster I will be referred to as "perfect cluster," and represents the ZnO crystal with no impurities and excitations. In clusters II and III, one-half electron has been removed from the O 2s and Zn 3d bands, respectively. According to Fig. 2, we interpret the highest valence band (O 2p) as a broad band for which the hole is delocalized. On the other hand, the Zn 3d and O 2s bands are narrow and their self-energy must be included in calculating the excitation energy.

ZnO doped with substitutional Cu in the ground state is described by cluster IV, and with substitutional Ni by cluster VII. Clusters V and VIII were used to calculate the internal 3d transitions for the 2+ impurity centers.

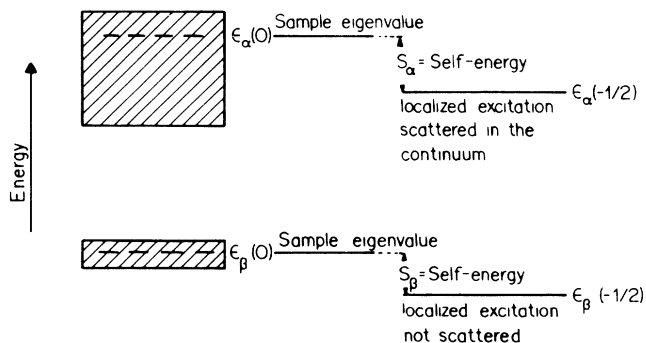


FIG. 2. Schematic representation of a single-particle excitation (hole) in a broad (upper part of the figure) or narrow band (lower part). For the narrow band case, the localized excitation is not scattered into the band continuum and is stationary (or quasi). In this case, the excitation energy should be calculated with the transition state, to account for the self-energy.

TABLE I. Geometric parameters for cluster calculations.

	R_i (a.u.)	γ_i
Central atom	1.995	1.0
1st neighbors	1.743	1.0
2nd neighbors	1.995	1.0
Outer sphere	8.099	-0.25

Cubic lattice parameter is 8.62

	Maximum angular momentum			
	a_1	t_2	t_1	e
Central atom	3	3	4	4
1st neighbors	2	2	2	2
2nd neighbors	1	1	1	1
Outer sphere	4	3	4	4

TABLE II. Calculated clusters and their configurations.

Cluster number	Formula	O 1s band	Zn 3d band	O 2p band	Impurity 3d band
I	ZnO ₄ Zn ₁₂	$1a_1^2 1t_2^6$	$2t_2^6 1e^4 e_{\text{ext}}^{120}$	$1t_1^6 2e^4 3t_2^6 2a_1^2 4t_2^6 3a_1^0$	
II		$1a_1^{1.5} 1t_2^6$	$2t_2^6 1e^4 d_{\text{ext}}^{120}$	$1t_1^6 2e^4 3t_2^6 2a_1^2 4t_2^6 3a_1^0$	
III		$1a_1^2 1t_2^6$	$2t_2^{5.5} 1e^4 d_{\text{ext}}^{120}$	$1t_1^6 2e^4 3t_2^6 2a_1^2 4t_2^6 3a_1^0$	
IV	CuO ₄ Zn ₁₂	$1a_1^2 1t_2^6$	d_{ext}^{120}	$(2t_2^6 1t_1^6 1e^4 3t_2^6) 2a_1^2$	$2e^4 4t_2^5$
V				$(2t_2^6 1t_1^6 1e^4 3t_2^6) 2a_1^2$	$2e^{3.5} 4t_2^{5.5}$
VI				$(2t_2^6 1t_1^6 1e^4 3t_2^6) 2a_1^{1.5}$	$2e^4 4t_2^{5.5}$
VII	NiO ₄ Zn ₁₂	$1a_1^2 1t_2^6$	d_{ext}^{120}	$(2t_2^6 1t_1^6 1e^4 3t_2^6) 2a_1^2$	$2e^4 4t_2^4$
VIII				$(2t_2^6 1t_1^6 1e^4 3t_2^6) 2a_1^2$	$2e^{3.5} 4t_2^{4.5}$
IX				$(2t_2^6 1t_1^6 1e^4 3t_2^6) 2a_1^{1.5}$	$2e^4 4t_2^{4.5}$

The possibility of transferring a hole from the d shell of the $2+$ impurity to an acceptor state is described using clusters VI and IX.

The degree of ionicity and charge transfer from Zn to O depends to a large extent on the amount of hybridization $O 2p \rightleftharpoons Zn 3d$. In a cluster calculation, the valence of Zn and O atoms is not that of an infinite crystal. For the clusters with 17 atoms, the hybridization results mainly from the interaction between the states $2t_2$ and $4t_2$ (cluster I). We found that a stable location of the Zn $3d$ states ($2t_2$ and $1e$, cluster I) could only be attained by eliminating the basis functions Zn $3d$ from the $4t_2$ wave function, so that hybridization was artificially truncated.

The energy levels at full occupation are shown in Fig. 3 for pure and doped ZnO. The upper valence bands are mainly derived from the O $2p$ state and the lowest conduction band from Zn $4s$. The levels were classified according to the irreducible representations of the T_d point group, and the zero of energy set at the highest valence-band (VB) state for the "perfect cluster." In this respect we recall that the "crystalline cluster" technique being used allows one to compare one-particle energies of different clusters because all have a unique energy reference.

The conduction and the O $2p$ valence bands are wide,^{17,18} thus the optical transition (OT₁) between them should be calculated using the Koopmans's theorem (no self-energy). In calculating the Zn $4s$ ($3a_1$) state that samples the conduction band, the Zn $4s$ basis function of the outermost Zn shell was eliminated because it is responsible for mixing the cluster surface states that we do not want. This procedure avoids the penetration of the conduction state into the outer region of the cluster. The calculated band gap is 5.65 eV, larger than the experimental 3.4 eV (as it should, according to the schematic Fig. 1) by a large factor because only the internal Zn atom is contributing. If the outermost Zn $4s$ basis functions are maintained the calculated gap becomes 2.9 eV, which is in an illusory good agreement with experiment.

The results displayed in Table III show the position and width of the ZnO bands compared to an experimental value¹¹ and band calculation values.^{17,8} Observe that in calculating the entries of the table, one takes the differences of eigenvalues calculated with different clus-

ters. If one compares the results for clusters II and III in Fig. 3 with the lower part of the schematic Fig. 2, one sees that the O $2s$ and Zn $3d$ bands are indeed "narrow" and the hole self-energy is an important part of the excitation energy. Lacking experimental values it is difficult

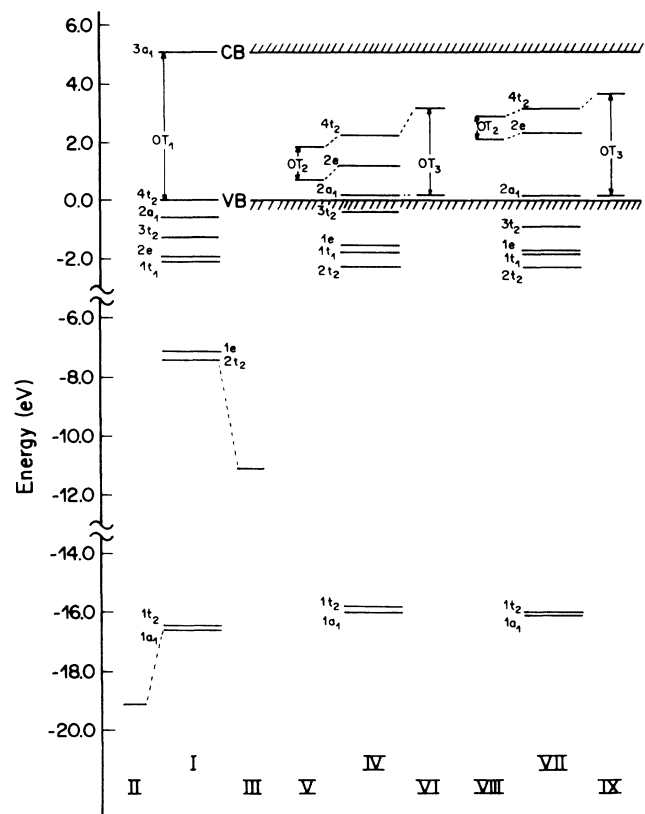


FIG. 3. Energy levels (a) at full occupation for clusters ZnO₄Zn₁₂ (I), CuO₄Zn₁₂ (IV), and NiO₄Zn₁₂ (VII); (b) for the transition states of the s and d valence bands (clusters II and III); (c) for the transition states defining the optical transitions OT₂ and OT₃ of the Cu²⁺ impurity (clusters V and VI); (d) for the transition states defining the optical transitions OT₂ and OT₃ of Ni²⁺ impurities (clusters VIII and IX). CB and VB are the conduction- and valence-band extrema, as defined in the cluster (see Fig. 1 for a comparison between the extrema for the crystal and for the cluster).

TABLE III. Energy differences for pure ZnO. ϵ_α^N is the eigenvalue for state α in cluster N (Table II). For the narrow bands, we use the eigenvalues at half-occupation.

	Configuration change	Energy	Calculated (eV)	Others (eV)
Band gap (OT ₁)	$4t_2^6 3a_1^0 \rightarrow 4t_2^5 3a_1^1$	$\epsilon_{3a_1}^I - \epsilon_{4t_2}^I$	5.65	3.4 ^a (expt)
O <i>s</i> band position	$1a_1^2 4t_2^5 \rightarrow 1a_1^1 4t_2^6$	$\epsilon_{4t_2}^I - \epsilon_{1a_1}^{II}$	18.60	20.68 ^{b,c}
Zn <i>3d</i> band position	$2t_2^6 4t_2^5 \rightarrow 2t_2^5 4t_2^6$	$\epsilon_{4t_2}^I - \epsilon_{2t_2}^{III}$	11.16	5.85 ^{b,c}
O <i>p</i> bandwidth	$1t_2^6 4t_2^5 \rightarrow 1t_1^5 4t_2^6$	$\epsilon_{4t_2}^I - \epsilon_{1t_1}^I$	2.1	1.52 ^{b,c}

^aReference 11.

^bReference 17.

^cReference 18.

TABLE IV. Optical transitions for ZnO with Cu and Ni impurities. ϵ_α^N is the eigenvalue for the state α in cluster N (Table II). The energy differences were calculated for the ground state cluster and for the cluster where one-half electron is promoted.

Optical transition (OT)	Configuration change	Energy	Calculated (eV)	Experiment (eV)
OT ₂ (Cu)	$(2e^4 4t_2^5) \rightarrow (2e^3 4t_2^6)$	$\epsilon_{4t_2}^V - \epsilon_{2e}^V$	1.21	0.72 ^a
		$\epsilon_{4t_2}^{IV} - \epsilon_{2e}^{IV}$	1.05	
OT ₃ (Cu)	$(2a_1^2 4t_2^5) \rightarrow (2a_1^1 4t_2^6)$	$\epsilon_{4t_2}^{VI} - \epsilon_{2a_1}^{VI}$	3.01	2.86 ^{a,b}
		$\epsilon_{4t_2}^{IV} - \epsilon_{2a_1}^{IV}$	2.06	
OT ₂ (Ni)	$(2e^4 4t_2^4) \rightarrow (2e^3 4t_2^5)$	$\epsilon_{4t_2}^{VIII} - \epsilon_{2e}^{VIII}$	0.88	0.51 ^a
		$\epsilon_{4t_2}^{VII} - \epsilon_{2e}^{VII}$	0.81	
OT ₃ (Ni)	$(2a_1^2 4t_2^4) \rightarrow (2a_1^1 4t_2^5)$	$\epsilon_{4t_2}^{IX} - \epsilon_{2a_1}^{IX}$	3.56	3.10 ^c
		$\epsilon_{4t_2}^{VII} - \epsilon_{2a_1}^{VII}$	3.05	

^aReference 26.

^bReference 22.

^cReference 20.

to decide whether the cluster or the band calculation has the best results.

Self-consistent cluster calculations were also performed for the substitutional Cu and Ni impurities. The impurity atom occupies the central site, as described by clusters IV and VII in Table II. In Fig. 3 we show the energy levels at full occupation for the 2+ impurities (clusters IV and VII). The 3*d* impurity levels are located in the gap region of the “perfect cluster” and split into *e* and *t*₂. An interesting feature is the introduction of a twofold degeneracy (spin degeneracy) *a*₁ acceptor state (deep trap) in the gap by the substitutional impurities. Our calculation indicates that this level is essentially (80%) an *sp*³ hybrid state. The 2*a*₁ state in the pure cluster I has this composition, indicating that the deep impurity trap is actually a host state.³¹ Table IV displays the main results of the impurity calculations. The optical transition OT₂ refers to

the infrared absorption spectrum observed for these impurities, and commonly assigned as an internal 3*d* transition of a 2+ ion. OT₃ represents a hole being transferred to one of the binding orbitals of the surrounding oxygen. This optical transition is the green luminescence decay of Cu and the blue luminescence of Ni. OT₂ and OT₃ were both calculated using the transition state and the Koopmans’s theorem, because we do not know how extended the wave functions are. The two sets of results do not differ much and are represented in Fig. 3.

To conclude we may say that a cluster calculation, if one is conscious of its limitations, can do much to the understanding of the electronic structure of semiconductors with and without impurities. It becomes especially useful in the calculation of localized one-particle excitations when the full machinery of the band Green function is computationally much too expensive.

- ¹L. G. Ferreira and M. L. DeSiqueira, *J. Phys. B* **16**, 311 (1983).
²W. V. M. Machado, L. G. Ferreira, and M. L. DeSiqueira, *J. Chem. Phys.* **71**, 4392 (1983).
³H. Chacham, M. L. DeSiqueira, L. G. Ferreira, and J. L. A. Alves, *J. Mol. Struct.* **120**, 207 (1985).
⁴D. L. Kinoshita, L. G. Ferreira, and M. L. DeSiqueira, *Int. J. Quantum Chem.* **28**, 85 (1985).
⁵W. V. M. Machado, L. G. Ferreira, and M. L. DeSiqueira, *J. Phys. B* **19**, 33 (1985).
⁶L. G. Ferreira, J. A. Kintop, and W. V. M. Machado, *J. Phys. B* **21**, 4063 (1988).
⁷L. M. Brescansin and L. G. Ferreira, *Phys. Rev. B* **20**, 3415 (1979).
⁸P. S. Guimaraes and L. G. Ferreira, *Rev. Bras. Fis.* **13**, 99 (1983).
⁹L. G. Ferreira and M. L. DeSiqueira, *Int. J. Quantum Chem. Symp.* **20**, 313 (1986).
¹⁰L. G. Ferreira and M. L. DeSiqueira, *Phys. Rev. B* **34**, 5315 (1986).
¹¹W. A. Harrison, *Electronic Structure and the Properties of Solids* (Freeman, San Francisco, 1980), p. 253.
¹²J. C. Phillips, *Rev. Mod. Phys.* **42**, 317 (1970).
¹³S. C. Abrahams and J. L. Bernstein, *Acta Crystallogr., Sect. B* **25**, 1233 (1969).
¹⁴U. Rossler, *Phys. Rev.* **184**, 733 (1969).
¹⁵D. G. Thomas, *J. Phys. Chem. Solids* **15**, 86 (1960).
¹⁶R. E. Dietz, J. J. Hopfield, and D. G. Thomas, *J. Appl. Phys. Suppl.* **32**, 2282 (1961).
¹⁷A. Kobayashi, O. F. Sankey, S. M. Volz, and J. D. Dow, *Phys. Rev. B* **28**, 935 (1983).
¹⁸J. R. Chelikowsky, *Solid State Commun.* **22**, 351 (1977).
¹⁹G. F. J. Garlick, in *Licht und Materie*, Vol. 26 of *Handbuch der Physik*, edited by S. Flugge (Springer-Verlag, Berlin, 1958), p. 29.
²⁰H. A. Wakliem, *J. Chem. Phys.* **36**, 2117 (1962).
²¹W. C. Holton, J. Schneider, and T. L. Estle, *Phys. Rev.* **133**, A1638 (1964).
²²R. Dingle, *Phys. Rev. Lett.* **23**, 579 (1969).
²³M. L. Reynolds, W. E. Hagston, and G. F. J. Garlick, *Phys. Status Solidi* **33**, 579 (1969).
²⁴M. L. Reynolds and G. F. J. Garlick, *Infrared Phys.* **7**, 151 (1967).
²⁵R. Baumert, I. Broser, U. W. Pohl, and B. Sange, *J. Phys. C* **18**, 4767 (1985).
²⁶H. J. Schulz and M. Thiede, *Phys. Rev. B* **35**, 18 (1987).
²⁷L. G. Ferreira and N. J. Parada, *Phys. Rev. B* **2**, 1614 (1970); *J. Phys. C* **4**, 15 (1971).
²⁸J. F. Janak, *Phys. Rev. B* **18**, 7165 (1978).
²⁹J. R. Leite and L. G. Ferreira, *Phys. Rev. A* **3**, 1224 (1971).
³⁰U. Lindefelt and A. Zunger, *Phys. Rev. B* **26**, 846 (1982).
³¹H. P. Hjalmarson, P. Vogl, D. J. Wolford, and J. D. Dow, *Phys. Rev. Lett.* **44**, 810 (1980).